On-body TOA-based ranging error model for motion capture applications within wearable UWB networks

Jihad Hamie, Benoit Denis, Raffaele D'Errico & Cedric Richard

Journal of Ambient Intelligence and Humanized Computing

ISSN 1868-5137

J Ambient Intell Human Comput
DOI 10.1007/s12652-013-0215-6

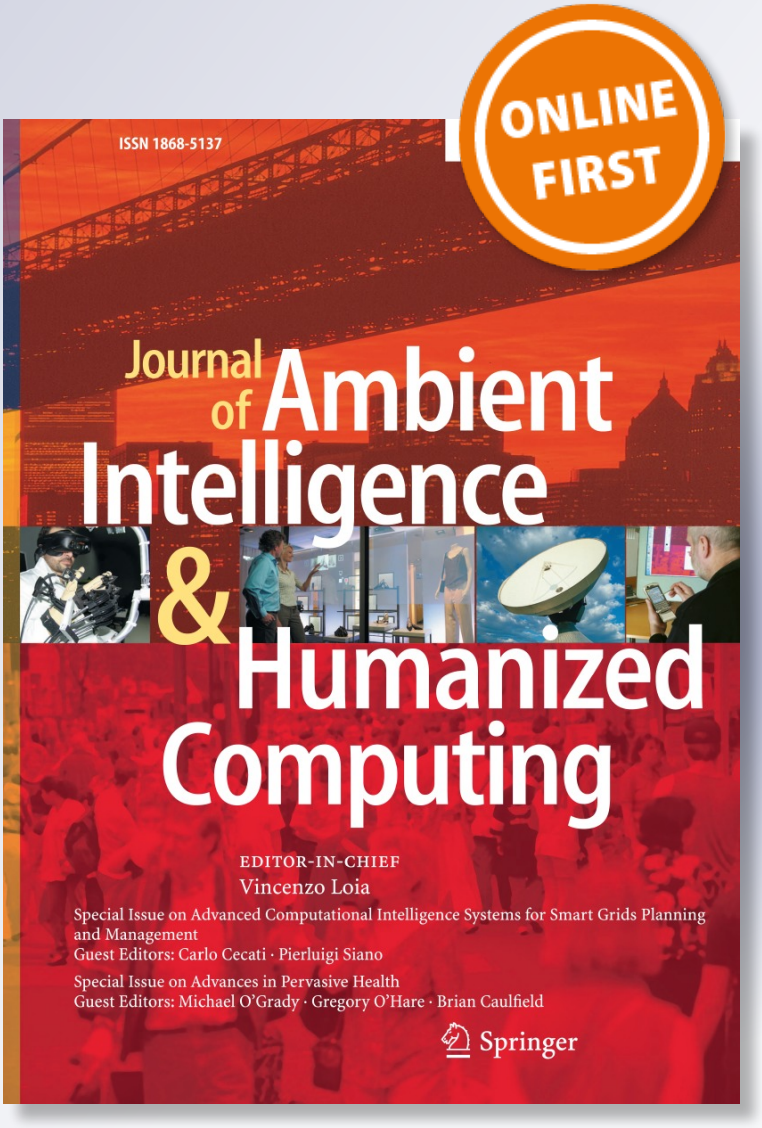

Springer

J Ambient Intell Human Comput
DOI 10.1007/s12652-013-0215-6

ORIGINAL RESEARCH

On-body TOA-based ranging error model for motion capture applications within wearable UWB networks

Jihad Hamie · Benoit Denis · Raffaele D'Errico · Cedric Richard

Received: 30 December 2012 / Accepted: 17 December 2013

Abstract We present herein an error model that characterizes on-body range measurements based on time of arrival (TOA) estimation in Impulse radio-ultra wideband, wireless body area networks. Considering real channel measurements over two representative on-body links for repeated walk cycles, the model is drawn as a conditional mixture, accounting for signal to noise ratio (SNR) variations and non line of sight (NLOS) channel obstructions caused by the body. Key model parameters are then investigated as a function of the previous obstruction and SNR configurations, illustrating missed/false path detection effects at low SNR. On this occasion, two TOA estimators are compared, namely a strongest path detection scheme through matched filtering and a first path detection scheme relying on high-resolution channel estimation. Finally, we discuss the possibility to generalize the previous model to any kind of on-body link, based on empirical observations regarding the dynamic range of the channel power transfer function under mobility. Accordingly, the resulting final model could integrate basic elements of classification, such as the instantaneous LOS/NLOS and static/dynamic link status.

J. Hamie (✉) · B. Denis · R. D'Errico
CEA-Leti Minatec Campus, 17 rue des Martyrs,
38054 Cedex 09 Grenoble, France
e-mail: hamiejihad@hotmail.com

B. Denis
e-mail: benoit.denis@cea.fr

R. D'Errico
e-mail: raffaele.derrico@cea.fr

C. Richard
Université de Nice Sophia-Antipolis/UMR CNRS 6525,
Parc Valrose, 06108 Cedex 2 Nice, France
e-mail: cedric.richard@unice.fr

Keywords Body shadowing · IEEE 802.15.6 · Impulse radio · Non line of sight · On-body propagation · Ranging error · Time of arrival · Ultra wideband · Wireless body area network

1 Introduction

Wireless body area networks (WBANs) are nowadays expected to fulfil the new technical requirements of various application fields such as healthcare, security, sports or entertainment Ullah et al. (2012), Ben Hamida et al. (2010), Kyung-Sup et al. (2010), Mekonnen et al. (2010), Shaban et al. (2010). The cooperative WBAN localization functionality consists in locating on-body nodes, relying on peer-to-peer range measurements. The latter can be performed over on-body radio links and/or possibly between nodes that belong to different WBANs. This add-on has been viewed as an important enabling feature for opportunistic large-scale human motion capture and/or coordinated group navigation applications. In this context, the Impulse radio-ultra wideband (IR-UWB) Gezici et al. (2005), Sahinoglu et al. (2008) benefits from fine multipath resolution capabilities for precise range measurements based on time of arrival (TOA) estimation. In the field of cooperative localization however, most of the algorithmic investigations carried out so far still consider unrealistic and synthetic TOA-based ranging errors under pedestrian mobility Ben Hamida et al. (2010), Mekonnen et al. (2010), Shaban et al. (2010), hence biasing somehow the performance assessment in practical operating conditions. In particular, as far as we know, there does not exist any ranging-oriented parametric model that can really account for dynamic UWB on-body links.

Published online: 25 December 2013

In this paper, we consider characterizing and modeling such TOA-based ranging errors, using representative UWB on-body channel measurements, which were carried out under typical pedestrian walking D'Errico and Ouvry (2009). More specifically, we take into account the dynamic link obstruction conditions experienced under body mobility, namely line of sight (LOS) and non line of sight (NLOS) conditions alternatively. The variation of the resulting model parameters is also studied and discussed as a function of a controlled signal to noise ratio (SNR) within synthetic received multipath signals. On this occasion, we illustrate false/missed first path detection phenomena under low SNR and NLOS conditions, as well as asymptotically ideal detections under higher SNR and LOS conditions. First peak and strongest peak detection schemes are then compared. Finally, based on the variations of the channel power transfer function observed over various on-body links, insights are also provided for an extension of the previous error model to any kind of links, based on the instantaneous LOS/NLOS and static/dynamic link status.

This paper is structured as follows. In Sect. 2, we introduce the on-body TOA-based ranging principle. Section 3 then presents the methodology adopted to generate realistic TOA estimates out of channel measurements and subsequent synthetic channels with controlled *SNR* values. In Sect. 4, we show the empirical probability density functions fitted to the resulting empirical errors, as well as the evolution of the related density parameters as a function of SNR and channel obstructions. Finally, Sect. 5 concludes the paper.

2 On-body TOA-based ranging

2.1 Single-link multipath channel

IR-UWB is a radio technology that makes use of non sinusoidal impulses Di Renzo et al. (2007). The main reasons motivating the use of IR-UWB in localization applications lies in its ability to provide high temporal resolution and accurate TOA estimation. Moreover, the IEEE 802.15.6 radio standard recently published for WBANs has promoted IR-UWB as a relevant physical layer in the very low power context Kyung-Sup et al. (2010). Typically, distances between on-body sensor nodes can be determined out of the TOA information, provided that n-way ranging protocol transactions are also used Sahinoglu et al. (2008). Then the resulting distance estimates usually feed localization or tracking algorithms to position the mobile nodes Destino et al. (2007). Finally, for the 3.1–5.1 and 3.75–4.25 GHz bands considered hereafter, it was previously shown in D'Errico and Ouvry (2009) that on-body channels suffer from significant shadowing, which is far dominating other distance-dependent effects. Accordingly, TOA estimation and its related error regimes are both expected to be strongly affected (and thus mostly conditioned) by dynamic body obstructions under mobility.

Over each on-body link, the received signal can be typically represented as a function of the transmitted signal as follows:

$$r(\tau) = \sum_{j=1}^{L_p} \alpha_j p(\tau - \tau_j) + n(\tau) = h(\tau) \otimes p(\tau) + n(\tau) \qquad (1)$$

where $h(\tau) = \sum_{j=1}^{L_p} \alpha_j \delta(\tau - \tau_j)$ is the multipath channel impulse response (CIR) if $\delta(.)$ is the Dirac delta function, L_p is the number of multipath components, α_j and τ_j are respectively the amplitude and delay of the j-th multipath component, $p(\tau)$ is the transmitted pulse and $n(\tau)$ is an additive noise process.

Out of this observed signal, the TOA estimation step aims at determining the arrival time of the direct multipath component that would be ideally received in a free space propagation case. As revealed by Eq. (1), the TOA estimation quality depends on multiple factors such as the emitted pulse energy (and hence, the received pulse energy) in comparison with the noise floor, multipath fading effects (and hence, the occupied bandwidth), or signal obstructions. It is thus possible to generate false alarms due to early noisy realizations or to miss the direct path due to poor SNR conditions and/or severe NLOS blockages. The latter tend to increase the apparent length of the direct path or they can even cause its absence, leading to overestimated ranges.

2.2 Detection schemes

2.2.1 Strongest peak detection

Matched filtering (MF) usually claims low complexity and low power consumption Shaban et al. (2010), which are particulary suitable features for WBAN applications. In our specific ranging context, TOA estimates are first obtained through strongest peak detection, by looking for the corresponding time shifts that maximizes the cross-correlation function between the received signal and a local template, which theoretically corresponds to the unitary transmitted waveform, as follows:

$$c(\tau') = \int_{-\infty}^{+\infty} r(\tau) p(\tau - \tau') \mathrm{d}\tau \qquad (2)$$

$$\hat{\tau}_{TOA} = \underset{\tau' \in W}{\operatorname{argmax}} |c(\tau')| \qquad (3)$$

where $c(\tau')$ is the cross correlation function, and $\hat{\tau}_{TOA}$ is the estimated TOA in the temporal observation window

W. The estimated distance is $\hat{d} = \hat{\tau}_{TOA} v$, where v is the speed of light, assuming that the transmitter and the receiver are somehow synchronized, e.g. through two way ranging protocol exchanges (i.e. assuming in first approximation that the time of flight (TOF) is equivalent here to the TOA reading and that the errors affecting TOF measurements are restricted to that affecting TOA measurements). It will be seen in the following how to cope in part with the actual timing uncertainty when characterizing estimation errors out of real channel measurements.

2.2.2 First path detection

Getting back to the CIR expression in Eq. (1), the propagation delay τ_j obviously reveals the physical length of the j-th corresponding path. Therefore, under LOS conditions where a direct path is truly present between the transmitter and the receiver, the shortest observable propagation delay can be reasonably associated with the true Euclidean distance. This method, which is depicted hereafter as the first arrival path (FAP) detection scheme, simply consists in preliminarily estimating the CIR out of the received signal $r(\tau)$ in Eq. (1), and to associate the first estimated multipath component (i.e. among all the resolved paths) with the estimated distance between transmitter and receiver. Unfortunately, in NLOS conditions, this FAP may suffer from significant power attenuations that makes it subject to missed/late detections or early false alarms, thus conducting to large estimation errors and, more generally speaking, to higher measurements dispersion. Many channel estimation algorithms have already been proposed to retrieve the CIR out of the received signals, such as finger selection (e.g. for RAKE receivers) or high resolution algorithms (e.g. CLEAN), as it will be seen in the next section.

In the sequel, the ranging error will be simply defined as the difference between the estimated TOA-based distance described previously and the actual distance, as follows:

$$e = \hat{d} - d \tag{4}$$

3 Error modeling methodology

This section describes the methodology adopted to draw our TOA-based ranging error model out of real channel measurements.

3.1 Multipath extraction from channel measurements

First of all, we consider the dynamic radio channels associated with the Hip-Chest and Hip-Wrist links from a past measurement campaign described in D'Errico and Ouvry (2009), where the total recording time was 4 sec and consecutive temporal channel responses were collected every 20 ms in the band 3.1–5.1 GHz. The measurements were performed under moderate human walk mobility in a typical indoor environment, resulting in a set of 200 time-stamped channel responses. For each response, multipath components were extracted using a CLEAN-like high resolution-algorithm Denis and Keignart (2003) in 3.1–5.1 GHz and (3.75, 4.25) GHz. A snapshot of the extracted CIR at the observation time-stamp t_n can hence be expressed as:

$$\hat{h}(t_n, \tau) = \sum_{j=1}^{\hat{L}_p(t_n)} \hat{\alpha}_j(t_n)\delta(\tau - \hat{\tau}_j(t_n)) \tag{5}$$

where $\hat{h}(t_n, \tau)$ is the CIR extracted at the observation time-stamp t_n, $\hat{L}_p(t_n)$ is the number of extracted multipath components, $\hat{\alpha}_j(t_n)$ and $\hat{\tau}_j(t_n)$ are respectively the amplitude and delay of the j-th extracted multipath component at time-stamp t_n.

Just like in D'Errico and Ouvry (2009), the dynamic power transfer function was also directly calculated out of the corresponding time-stamped frequency-domain measurements $H(t, f)$ in the band B (anyway made available for RF calibration purposes), as follows:

$$P(t_n) = \frac{1}{b}\int_B |H(t_n, f)|^2 \mathrm{d}f \tag{6}$$

where b is the bandwidth of B, and $P(t_n)$ is the time-variant power transfer function, as illustrated on Fig. 1 for the Hip-Wrist link.

As expected, this figure shows the strong body obstruction effects on the received signal attenuation. Typically NLOS channel conditions periodically lead to severe fades due to body shadowing under mobility.

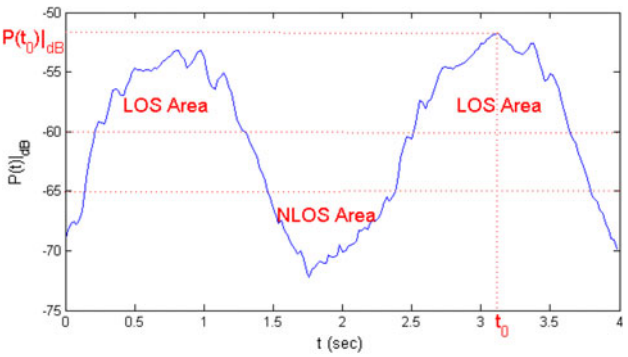

Fig. 1 Dynamic variations of the power transfer function between the hip and the wrist under body mobility (standard walk), as a function of time t

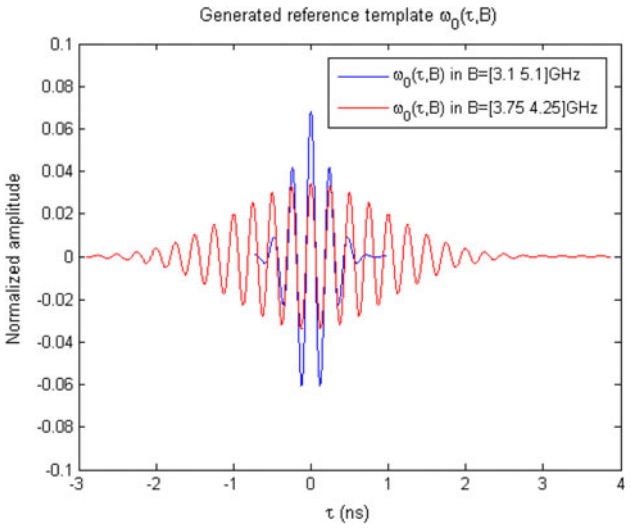

Fig. 2 Energy-normalized templates $w_0(\tau,B)$ used for the generation of synthetic received signals and for correlation-based TOA estimation

3.2 Generation of synthetic received signals

In order to synthesize a realistic received signal out of the extracted CIRs, as a function of a given initial SNR level and occupying a given bandwidth, a reference template waveform is required. Gaussian-windowed sine waves have thus been generated in the 3.1–5.1 and 3.75–4.25 GHz bands, the latter being in compliance with one mandatory band specified by the IEEE 802.15.6 bandplan. Figure 2 shows the corresponding reference templates normalized in energy. According to equation (1), those templates shall be convolved with the CIRs previously extracted out of real measurements, and an additive white Gaussian noise (AWGN) process with a two-sided power spectral density N_0 (i.e. $N_0 = -154$ dBm/Hz) is filtered into the considered signal band. The resulting synthetic received signal available at the observation time-stamp t_n is thus given by:

$$\begin{aligned} W_s(t_n,\tau) &= \hat{h}(t_n,\tau) \otimes w_0(\tau,B) + n(t_n,\tau,B) \\ &= \sum_{j=1}^{\hat{L}_p(t_n)} \hat{\alpha}_j(t_n) w_0(\tau - \hat{\tau}_j(t_n), B) \\ &\quad + n(t_n,\tau,B) \end{aligned} \tag{7}$$

where $w_0(\tau,B)$ is the reference template and $n(t_n, \tau, B)$ is the band-limited noise process at the observation time-stamp t_n in the occupied band B.

For our simulation needs, in order to enable a dynamic variation of $SNR(t_n)$ and to preserve the natural relative power fluctuations due to body obstructions (as observed during the measurements campaign), we set and control the SNR values a priori for an arbitrary reference time stamp (preferably in LOS). In our case, the reference time t_0 is for instance chosen when the received channel exhibits a maximum of the power transfer function $P(t)$. Imposing a priori the reference value $SNR(t_0)$ (as an input parameter) and given the actual $P(t_n)$ [and hence $P(t_0)$] directly available from measurements at any time-stamp t_n, the instantaneous $SNR(t_n)$ is then forced and scaled artificially so as to vary realistically over the entire acquisition duration, as follows:

$$SNR(t)|_{dB} = SNR(t_0)|_{dB} + P(t)|_{dB} - P(t_0)|_{dB} \tag{8}$$

where $SNR(t)$ is the re-scaled instantaneous signal energy to noise ratio, $SNR(t_0)$ and $P(t_0)$ are respectively the controlled SNR value and power transfer function at time-stamp t_0, and $P(t)$ is the power transfer function at time t. In our study, $SNR(t_0)$ is viewed as in imposed input parameter, which remains constant and valuable for the whole duration of one walk cycle, and over several noise process realizations (i.e. over which statistics are drawn). Practically, before applying (8) to account for the overall walk duration from the reference time stamp t_0, given the fixed filtered noise power imposed by B and N_0, we re-scale the synthetic multipath impulse response $\hat{h}(t_0,\tau)$ in (7) into $\hat{h}_r(t_0,\tau)$ so that $W_{s,r}(t_0,\tau) = \hat{h}_r(t_0,\tau) \otimes w_0(\tau,B) + n(t_0,\tau,B)$ can respect the input parameter $SNR(t_0)$ (and thus, applying the same scaling factor to the useful signal for each random noise process realization), as follows:

$$SNR(t_0)|_{lin} = \frac{\int [W_{s,r}(t_0,\tau') - n(t_0,\tau',B)]^2 d\tau'}{N_0} \tag{9}$$

The rationale for parameterizing the error model with $SNR(t_0)$ are twofold: (1) we have noticed that the error regime is rather stable over LOS or NLOS portions of a given walk (i.e. exhibiting approximately the same statistics under relatively small variations of the instantaneous SNR) but mostly conditioned on body shadowing and (2) $SNR(t_0)$ shall be easier to predict once for all at the beginning of the walk cycle in localization-oriented simulations (e.g. with classical free-space propagation models) for being advantageously associated with LOS conditions.

3.3 Emulated TOA estimates and conditional error regimes

At each observation time-stamp t_n, TOA estimates are thus estimated from each synthesized noisy received signal, using two kinds of estimators. The first one consists of a matched filter, as described in Sect. 2.2.1, i.e. by looking for the time shift that maximizes the cross-correlation function between the synthetic received signal $W_{s,r}(t_n, \tau)$

and the reference template $w_0(\tau, B)$, within a given observation. In our case, the window has a time length of 5 *ns* like in Di Renzo et al. (2007), Shaban et al. (2010). This duration is sufficient to observe an arrival time corresponding to the maximum distance between two synchronized nodes placed on the same body.

The second TOA estimate is based on FAP detection using a CLEAN-like approach, which can be shortly described for each time stamp t_n as follows Yang (2004):

(1) Calculate the self-correlation $r_{w_0w_0}(t_n, \tau)$ of the template and the cross-correlation $r_{w_0W_s}(t_n, \tau)$ of the template with the synthesized received signal $W_s(t_n, \tau)$.
(2) Find the largest correlation peak in $r_{w_0W_s}(t_n, \tau)$, record the normalized amplitude α_k and the relative time delay τ_k of the correlation peak.
(3) Subtract $r_{w\_0}w_0(t_n,\tau)$ scaled by α_k from $r_{w\_0}W_s(t_n,\tau)$ at the time delay τ_k.
(4) If a stopping criterion (e.g. a minimum threshold on the peak correlation) is not met, go to step 2. Otherwise, stop.
(5) The overall CIR $\widehat{h}(t_n, \tau)$ is extracted, and the FAP is recorded as the first in time resolved multipath component $\widehat{\tau}_1(t_n)$.

The first Hip-Chest link to be considered is always assumed in LOS conditions, whereas the Hip-Wrist link varies dynamically, leading periodically and alternatively to LOS and NLOS conditions. In order to classify the obstruction conditions, the retained method is based on the power transfer function. Relying on the initial measurements, the channel is considered in LOS (resp. NLOS) conditions whenever its power transfer function is larger (resp. lower) than −60 dB (resp. −65 dB). The remaining unspecified time area is considered as a transition zone, with a steep power transition regime. Alternatively, the channel delay spread, which exhibits smaller values in LOS and higher values in NLOS conditions, could have been used to identify the channel obstruction configurations.

Finally, during the initial communication-oriented measurement campaign reported in D'Errico and Ouvry (2009), the real distance between nodes was not collected, since measurements were not carried out for localization purposes. However, in first approximation, one can try to extract this distance out of the measured TOA in time-stamp regions when the LOS conditions are clearly identified and with $SNR(t_0) = +\infty$ for the synthetic received signals in the largest bandwidth 3.1–5.1 GHz. Practically, the first Hip-Chest link is considered as fixed and the reference distance extraction was directly realized by averaging all the TOA measurements issued from MF estimation over the walk cycle to reduce TOA estimation errors appeared during the multipath extraction phase in the presence of overlapping components. Nevertheless, for the second Hip-Wrist link, a smoothing process was performed in a sliding window whose length corresponds to 20 consecutive time-stamp samples (e.g. within 20 × 20 ms = 400 ms). The true distance was subsequently interpolated over NLOS areas, assuming continuity of the true distance at LOS/NLOS boundaries but discontinuity for the smoothed version of the measured distance (obtained with the sliding window). The idea consists in relying on the known extracted LOS portions, thus forming a time-stamp basis to infer the true distance in unknown NLOS time-stamp areas through spline-based data extrapolation. Figure 3 intends to clarify the method used to determine the reference distance, assuming the latter will correspond to the so-called "expected real" distance while computing the ranging error in the following.

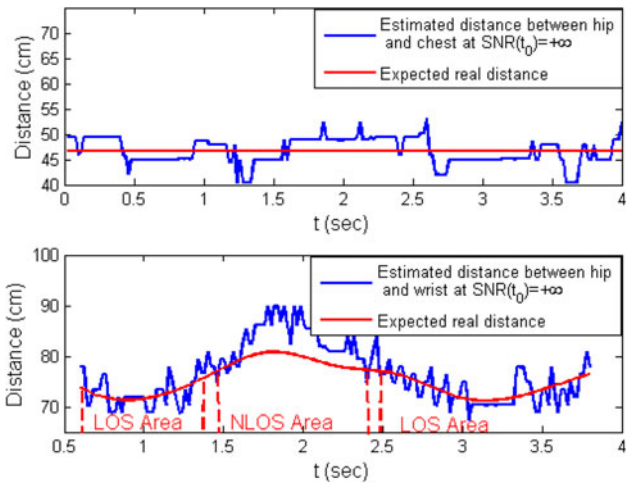

Fig. 3 Equivalent inter-node distance retrieved out of correlation-based TOA estimation without noise (*blue*) and fitted reference distance after averaging with a sliding window and splines interpolation over the detected NLOS time stamp region (*red*), for both Hip-Chest (*top*) and Hip-Wrist links (*bottom*) (color figure online)

4 Results

In this section we statistically characterize the obtained TOA-based ranging errors carried out of matched filter estimator, in the 3.1–5.1 and 3.75–4.25 GHz frequency bands, for the two kinds of radio links. As previously mentioned, these models are conditioned on the channel obstruction status and on the reference $SNR(t_0)$. While running simulations, for each $SNR(t_0)$ value, 100 independent noise process realizations are drawn for the walk cycle duration. Over these realizations, for each frequency band, up to 20,000 range measurements are then collected

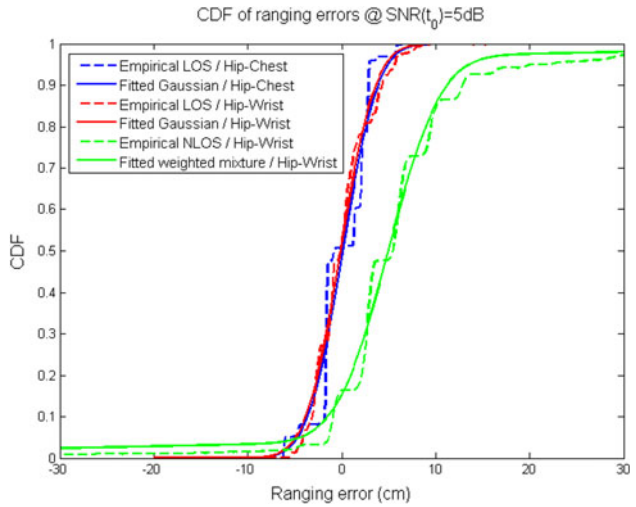

Fig. 4 Empirical and model-based CDFs of ranging errors with a matched filter TOA estimator (i.e. strongest path detection), in both LOS and NLOS conditions, with $SNR(t_0) = 5$ dB, in the band 3.1–5.1 GHz

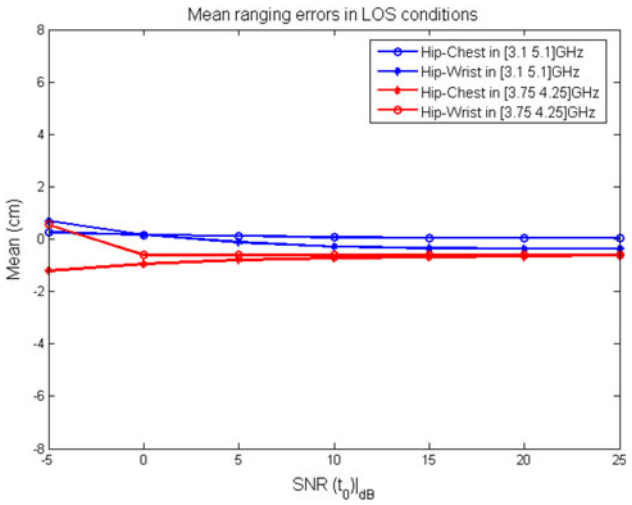

Fig. 5 Mean of ranging errors with a matched filter TOA estimator (i.e. strongest path detection), in LOS conditions, as a function of $SNR(t_0)$

in LOS conditions for the Hip-Chest link, whereas 8600 and 3,800 measurements are generated for the Hip-Wrist link, respectively in LOS and NLOS conditions. Moreover, we draw the model of the TOA-based ranging errors carried out of FAP detection using a CLEAN algorithm, in 3.1–5.1 GHz frequency band, for the two kinds of radio links, but only under LOS conditions, while the FAP is almost missed or false detected in NLOS conditions.

4.1 LOS model

4.1.1 Strongest path detection

Conditioned on the LOS case, it appears that the step-wise empirical cumulative density function (CDF) of emulated range measurements enjoys a rather satisfactory fit (in a least squares sense) to the CDF of a Gaussian random variable, whose standard deviation σ is on the order of the time base period. Figure 4 shows examples for both simulation-based and model-based LOS CDFs with $SNR(t_0) = 5$ dB in the band 3.1–5.1 GHz.

Figures 5 and 6 show respectively the variations of the mean and standard deviation of the corresponding Gaussian LOS model for both links and both bands, as a function of $SNR(t_0)$. As seen in Fig. 5, the mean varies around zero, with very low values (in comparison with the nominal expected true range value), and hence, it can be considered as null in first approximation over the explored range of $SNR(t_0)$ values. Figure 6 shows that the behavior of the standard deviation is asymptotically constant when $SNR(t_0)$ reaches a value of 10 dB. At high

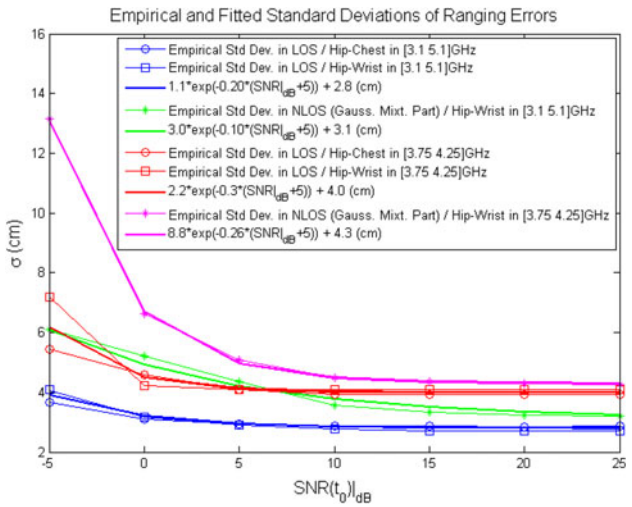

Fig. 6 Standard deviations of ranging errors σ with a matched filter TOA estimator (i.e. strongest path detection), in LOS and NLOS conditions, as a function of $SNR(t_0)$

SNRs, the strongest path detected through cross-correlation indeed coincides systematically with the direct path. The asymptotic error floor at high SNR thus depends mostly on the occupied band and center frequency, as discussed in Sahinoglu et al. (2008).

To summarize, considering the tested Hip-Chest and Hip-Wrist links, the distribution of the ranging error through correlation-based TOA estimation in LOS conditions in the 3.1–5.1 and 3.75–4.25 GHz bands can be simply modeled as a centered Gaussian distribution, with a standard deviation depending on B and $SNR(t_0)$ (see the legend of Fig. 6 for detailed model parameters).

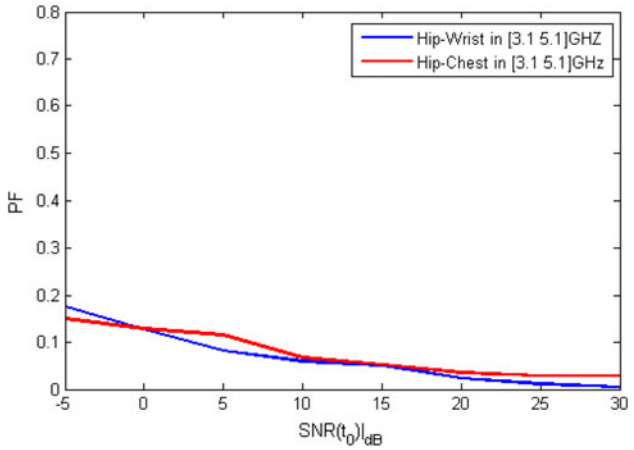

Fig. 7 Variation of the false alarm probability for FAP TOA estimation (i.e. first path detection), using a threshold of 10 dB below the global absolute maximum of the estimated CIR, in LOS conditions, in the band 3.1–5.1 GHz, as a function of $SNR(t_0)$

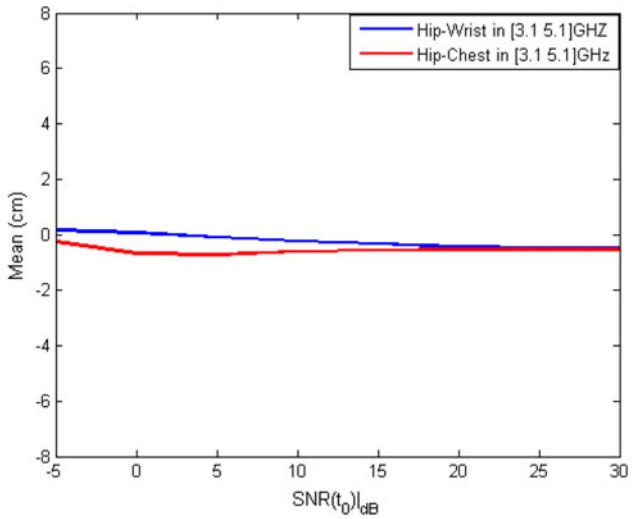

Fig. 8 Mean of ranging errors for FAP TOA estimation (i.e. first path detection), in LOS conditions in the band 3.1–5.1 GHz, as a function of $SNR(t_0)$

4.1.2 First path detection

For TOA estimation through FAP detection, the resulting probability density function (PDF) can be better represented by a mixture involving Gaussian and Uniform components. The Uniform distribution in involved is weighted by the false alarm probability *PF*, which represents the probability to detect a wrong peak earlier than the true FAP. *PF* is thus strongly affected by the threshold chosen within the FAP detection scheme (e.g. a smaller threshold obviously leads to higher *PF*), and hence, by the stopping rule in the underlying high-resolution channel estimation algorithm. Figure 7 shows the variation of PF as a function of $SNR(t_0)$ for both links in the 3.1–5.1 GHz

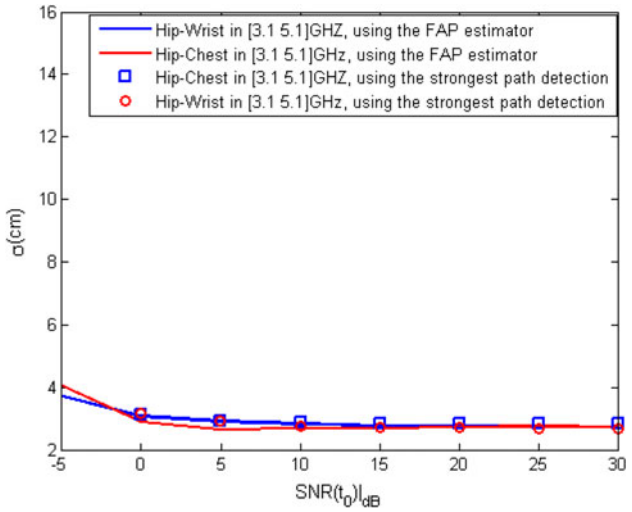

Fig. 9 Comparison between the variations of the standard deviations of ranging errors σ using a FAP TOA estimator (i.e. first path detection using a threshold of 10 dB below the global absolute maximum of the estimated CIR) and strongest correlation peak TOA estimator, in LOS conditions, in the band 3.1–5.1 GHz, as a function of $SNR(t_0)$

frequency band. At high $SNR(t_0)$, the behavior appears to be almost Gaussian and *PF* is approximately zero. Figures 8 and 9 show respectively the variations of the mean and standard deviation of the corresponding Gaussian distribution, for both links in the band 3.1–5.1 GHz. These variations are compliant with the variations observed in the matched filter case in case of strongest path detection. This result shows that, in general LOS conditions, the FAP is rather in line with correlation-based TOA estimation. Thus one would tend to apply systematic strongest path detection for low complexity in such favorable conditions.

4.2 NLOS model

As previously pointed out, in NLOS conditions (i.e. under body shadowing), the first path detection scheme being subject to much higher deviations, we mainly focus hereafter on the strongest path detection. The best fit has then been also obtained to a mixture-based model involving Gaussian and Uniform components. Figure 4 shows examples of both the empirical and model-based NLOS CDFs at $SNR(t_0) = 5$ dB, in the 3.1–5.1 GHz band.

The corresponding conditional PDF is then expressed as follows:

$$p(e) = \psi U(T_w) + (1 - \psi)G(\mu, \sigma^2) \tag{10}$$

where p is the PDF of the ranging error e in NLOS conditions, $U(T_w)$ is a uniform distribution, whose temporal support T_w depends on the receiver observation window while performing TOA estimation through cross-correlation. Again, this window is chosen to enable detection

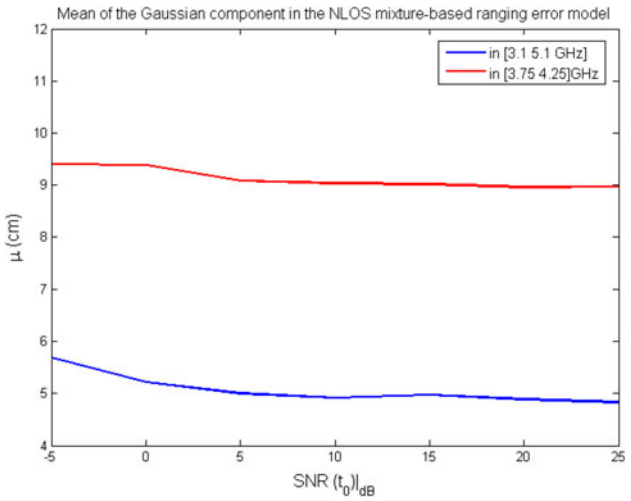

Fig. 10 Mean value associated with the Gaussian part of the ranging error mixture-based model in NLOS conditions, as a function of $SNR(t_0)$

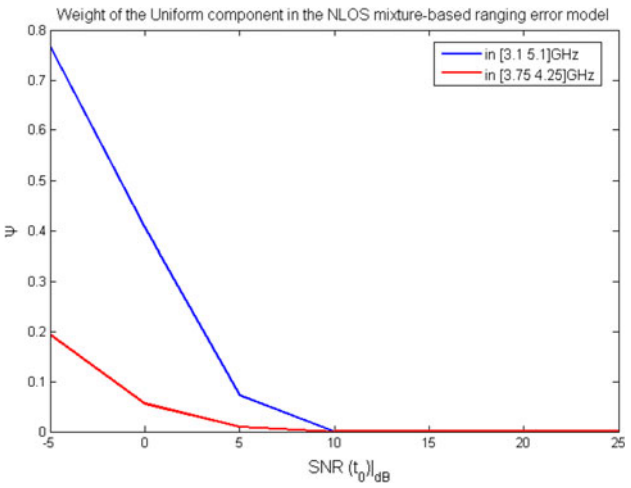

Fig. 11 Weight of the Uniform part of the mixture-based ranging error model in NLOS conditions, as a function of $SNR(t_0)$

within any on-body link after synchronization (e.g considering typically a worst case distance of 1.5m), ψ is the weight of the uniform distribution, and $G(\mu, \sigma^2)$ is a Gaussian distribution with a mean μ and a variance σ^2.

The variation of those parameters in both bands of interest, as a function of $SNR(t_0)$ is represented in Figs. 6, 10 and 11.

As shown on Fig. 11, at low $SNR(t_0)$, the contribution of the uniform distribution component is high. This effect accounts for the distribution of the so-called apparent path arrival determined through cross-correlation over the entire observation window (e.g. between 0 and 5 *ns*), when the noise level is so high that it can cause frequent missed detections or false alarms. The uniform weight in the mixture then directly reflects the probability of having either a false alarm or a missed detection. However, at higher $SNR(t_0)$, the behavior is almost Gaussian, where the ranging error is centered around a positive mean, which can be interpreted as a positive bias caused by the obstruction of the direct path (and hence, its apparent length extension). As shown in Figure 6, at high $SNR(t_0)$ (i.e. larger than 10 dB), in each operating band, the behavior of the error standard deviation in LOS is similar to the standard deviation of the Gaussian part of the mixture-based NLOS model, as the uniform weight is becoming quasi-null. Similar standard deviations means that the path detection performances are thus equivalently good in terms of dispersion in LOS and NLOS conditions, given the observed strongest path. However, it is worth keeping in mind that the apparent time of flight of the first observable path in NLOS cases is shifted independently of the path power, hence leading to a non-neglected ranging bias (i.e. besides random noise terms). The fact that the NLOS bias is approximately constant over $SNR(t_0)$ for a given band is also in line with the previous remarks. This very bias value, which seems to depend mostly on the occupied band, is rather hard to predict (as a deterministic parameter) and characterize further in practice. Hence, we recommend in our final ranging error model to assume this bias as a Uniformly distributed random variable, drawn once for all within a plausible range of a few tens of cm (i.e. approximately constant over all the NLOS portions of one given walk cycle).

4.3 Model generalization to other on-body links

Since our described model considers the dynamic channel variations and preserves the natural relative power fluctuations due to body obstructions (i.e. for NLOS) over two representative on-body links (i.e. Hip-Wrist and Hip-Chest), it is worth illustrating the variation of the power transfer function over other on-body links. Relying on the same channel measurements campaign from D'Errico and Ouvry (2009), which has been briefly introduced in Sect. 3.1, we have calculated the time-stamped power transfer function $P(t)$ over two additional dynamic on-body links for which the true distance was unknown (i.e. Hip-Thigh and Hip-Foot), with the transmitters and the receivers placed as on Fig. 12. Figure 13 then shows the dynamic variations of $P(t)|_{\mathrm{dB}}$ over these four on-body links, for both 3.75–4.25 and 3.1–5.1 GHz frequency bands. As it can be seen, $P(t)|_{\mathrm{dB}}$ spans approximately in the same range for all the dynamic links (i.e. Hip-Wrist, Hip-Thigh and Hip-Foot). Moreover, the static link (i.e Hip-Chest) is characterized by a relatively stable $P(t)|_{\mathrm{dB}}$ value as a function of the time stamp. The level is then approximately similar to that computed for dynamic links but restricted into their LOS areas. The previous observations indicate that the power transfer

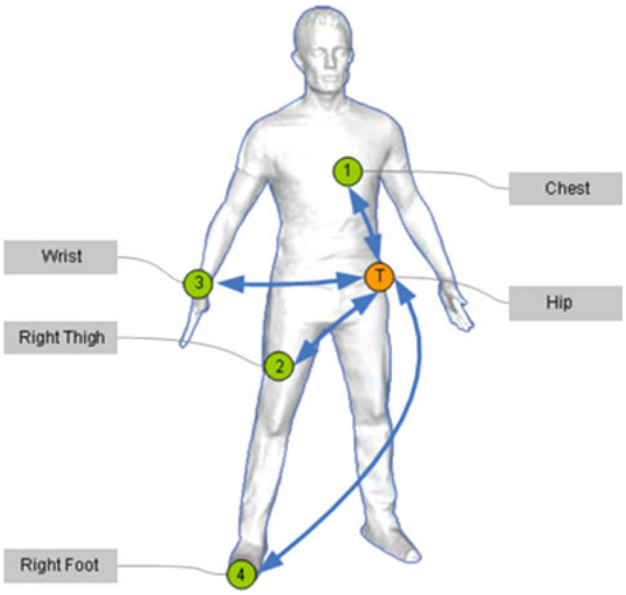

Fig. 12 Scenario of the on-body measurements campaign carried out in D'Errico and Ouvry (2009), including four star links

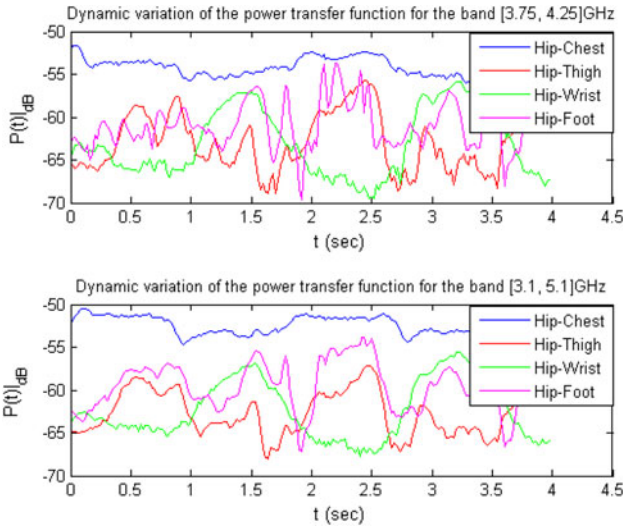

Fig. 13 Dynamic variation of the power transfer function for 4 on-body links, in both frequency bands 3.75–4.25 GHz (*top*) and 3.75–4.25 GHz (*bottom*)

function rely mostly on the channel obstruction conditions and the dynamic range of investigated values is approximately the same though rather independent from the used dynamic links. Moreover, those results are also compliant with a previous remark about the relative stability of the ranging error over LOS and NLOS portions of a given walk. Finally, it is clear that $P(t)|_{\mathrm{dB}}$ plays a critical role (through SNR normalization) with respect to the ranging error model parameters. Overall, it thus seems that the proposed error model, which has been based so far on two representative on-body links only, could be reasonably extended to other kinds of links experiencing similar power transfer conditions, being uniquely based on the LOS/NLOS and static/dynamic channel classifications.

5 Conclusion

In this paper we have characterized and modeled dynamic on-body ranging errors based on TOA estimation in the 3.1–5.1 and 3.75–4.25 GHz frequency bands, the latter band being compliant with the mandatory band plan proposed in the IEEE 802.15.6 standard. The drawn models are based on preliminary WBAN channel measurements performed in the band 3.1–5.1 GHz, conditioned on the channel obstruction configurations (i.e. LOS/NLOS). We have shown that the ranging error distribution could be modeled as a centered Gaussian distribution in LOS conditions in case of systematic strongest path detection, and as a weighted mixture between uniform and Gaussian distributions in the case of first path detection. Moreover, in NLOS conditions, ranging error is also modeled as as a weighted mixture between uniform and Gaussian distributions in the case of the TOA estimation through the strongest path detection, accounting for false alarms and missed detections. Considering the dynamic range of the channel power transfer function empirically observed for different nodes placements, a possible extension of the model to other on-body links has also been briefly proposed and discussed for further simulation convenience (i.e. in case of arbitrary on-body nodes deployment).

In future works, this model shall be used to realistically assess the performance of new positioning and tracking algorithms, addressing the still challenging problem of opportunistic large-scale individual motion capture based on stand-alone WBAN solutions.

Acknowledgments This work has been carried out in the frame of the CORMORAN project, which is funded by the French National Research Agency (ANR) under the contract number ANR-11-INFR-010.

References

Ben Hamida E, Maman M, Denis B, Ouvry L (2010) Localization performance in wireless body sensor networks with beacon enabled mac and space-time dependent channel model. In: Personal, indoor and mobile radio communications workshops (PIMRC Workshops), 2010 IEEE 21st International Symposium, pp 128–133

Denis B, Keignart J (2003) Post-processing framework for enhanced uwb channel modeling from band-limited measurements. In: Ultra wideband systems and technologies, 2003 IEEE Conference, pp 260–264

D'Errico R, Ouvry L (2009) Time-variant ban channel characterization. In: Personal, indoor and mobile radio communications, 2009 IEEE 20th International Symposium, pp 3000–3004

Destino G, Macagnano D, Abreu G, Denis B, Ouvry L (2007) Localization and tracking for ldr-uwb systems. In Mobile and Wireless Communications Summit, 2007, IEEE. 16th IST, pp 1–5

Di Renzo M, Buehrer R, Torres J (2007) Pulse shape distortion and ranging accuracy in uwb-based body area networks for full-body motion capture and gait analysis. In: Global telecommunications conference, 2007. GLOBECOM'07. IEEE, pp 3775–3780

Gezici S, Tian Z, Giannakis G, Kobayashi H, Molisch A, Poor H, Sahinoglu Z (2005) Localization via ultra-wideband radios: a look at positioning aspects for future sensor networks.In: Signal processing magazine, IEEE, 22(4):70–84

Kyung-Sup K, Ullah S, Ullah N (2010) An overview of ieee 802.15.6 standard. In: Applied sciences in biomedical and communication technologies (ISABEL), 2010 3rd International Symposium, pp 1–6

Mekonnen Z, Slottke E, Luecken H, Steiner C, Wittneben A (2010) Constrained maximum likelihood positioning for uwb based human motion tracking. In: Indoor positioning and indoor navigation (IPIN), 2010 International Conference, pp 1–10

Sahinoglu Z, Gezici S, Guvenc I (2008) Ultra-wideband positioning systems: theoretical limits, ranging algorithms, and protocols. Cambridge University Press, Cambridge

Shaban H, El-Nasr M, Buehrer R (2010) Toward a highly accurate ambulatory system for clinical gait analysis via uwb radios. Inf Technol Biomed IEEE Trans 14(2):284–291

Ullah S, Higgins H, Braem B, Latre B, Blondia C, Moerman I, Saleem S, Rahman Z, Kwak K (2012) A comprehensive survey of wireless body area networks. J Med Syst 36(3):1065–1094

Yang L (2004) The applicability of the tap-delay line channel model to ultra wideband. PhD thesis, Virginia Polytechnic Institute and State University